Proceedings of the Turin Royal Academy of Science
Vol. 79, 1944

WIRE ROPE BENDING STIFFNESS FACTORS

By Modesto Panetti
Introduction and translation from Italian
by Alain Cardou, Ph.D.

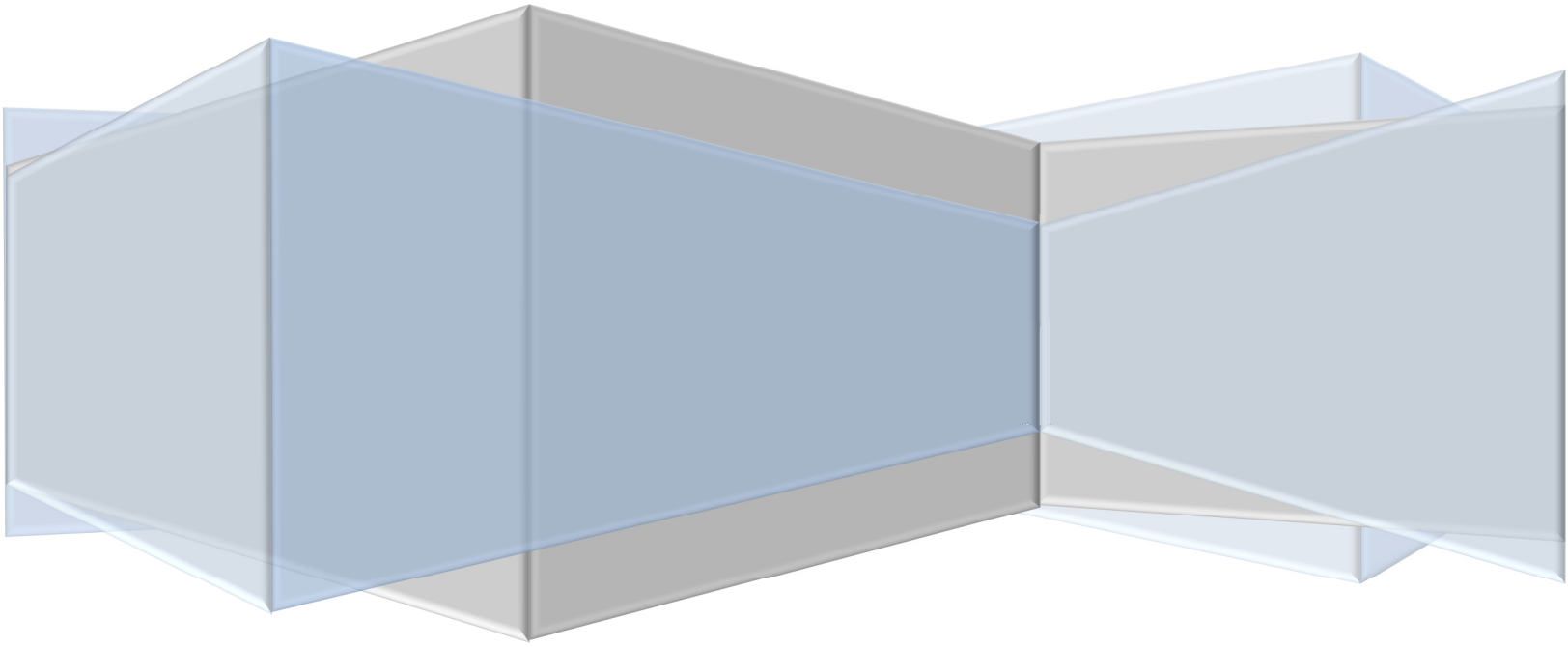

WIRE ROPE BENDING

STIFFNESS FACTORS

By

Modesto Panetti

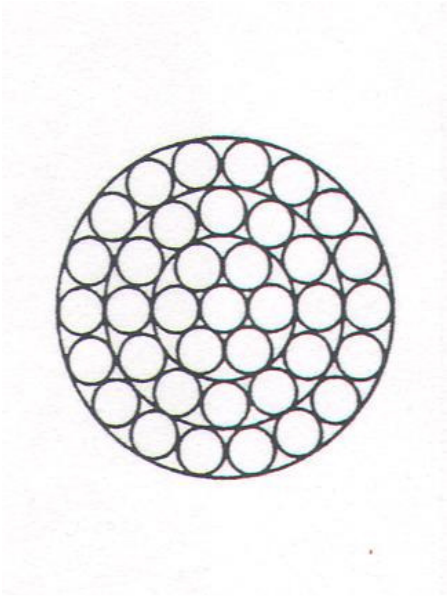

Translated from Italian
by
Alain Cardou, Ph.D.
2015

MODESTO PANETTI (1875-1957)

An Italian engineer, he became Applied Mechanics professor in Genoa and, later, in Torino. Member of the Turin Academy of Science, of the Papal Academy of Science, and corresponding member of the "Accademia dei Lincei" (of which Academy Galileo Galilei was an early member). A Senator and also Minister of Postal Service and Telephone after World War II

FOREWORD

Helical strand mechanics may apply to such practical systems as cables and overhead electrical conductors. In a 1997 review paper, Cardou and Jolicoeur summarized current available models[1] . In 2006, this review has been updated by Cardou, at least for the bending stiffness problem[2].

In the latter, several early contributions were mentioned, which had been "forgotten" in the 1997 review. Among them, a paper by Panetti (1944), published in Italian and, probably for that reason, completely ignored in the later technical literature. The translation given below strives to redress as much as possible this "injustice".

Of course, one may wonder if Panetti's results are still relevant. In recent years, several studies have been published which were based on the Finite Element method. In general, they deal with the relatively simple axial load problem. A multilayer strand in bending is much more complex a problem, involving multiple contact points (at least for cross-lay strand), friction, partial slip etc. Thus, a numerical treatment will obviously necessitate a number of simplifying assumptions. For that reason, an analytical approach is still of interest.

Analytical models also require a number of assumptions, and Panetti's are not immune to criticism, such as his hypothesis of "circumferential" or same layer contact between wires. However, his uniform curvature bending stiffness theory yields, at least qualitatively, similar results to more recent models.

Panetti's paper can therefore be read with interest by anyone working on a new model of helical strand mechanics. In any case, it should deserve proper credit through its inclusion in relevant lists of references.

A.C.

[1] Cardou, A., and Jolicoeur, C., *Mechanical models of helical strands*, Applied Mechanics Reviews, Vol. 50, No 1, pp. 1-14.
[2] Cardou, A., *Taut helical strand bending stiffness*, available on line at www.umformtechnik.net. 9 pages

WIRE ROPE BENDING STIFFNESS FACTORS

A presentation[3] by Modesto Panetti
(Member of the Academy)

Presented at the 23 February 1944 Meeting

ABSTRACT

First, cable geometry is presented. Then, interwire pressure arising from the applied axial load is derived. It is based on the "circumferential contact" assumption, as opposed to the more widely used "radial contact" assumption, which was used even by the Author himself in a previous paper on the same subject.

This assumption yields a simpler calculation of friction work occurring in a taut cable in bending, where the limit case of inextensible wire is made, and also that of bending tensile forces, whose determination is based on the theoretical case of a uniform curvature.

This approach allows a separate study of the stiffness factors and of bent cable debonding from the cable bending details, such as its deformed curve geometry, as they appear in previous papers by Findeis and Hellmut Ernst.

This presentation concludes by deriving a relationship between curvature and resisting internal moments. The corresponding equation might be of some practical interest in applications.

INTRODUCTION

If curvature is imposed onto a wire rope under axial load, supplementary forces are generated in individual wires. Depending on the location of a wire section with respect to the cable neutral axis, they add up or subtract from the initial wire tensile force.

At the same time, tangential forces are generated between contacting wires. They arise from two separate phenomena.

Firstly, they will come from the variation of cable curvature along its axis. It is equivalent to shear stress generation in a solid beam in bending.

Secondly, they arise from the helical winding of wires, even under uniform curvature. For a taut cable, such a uniform curvature may be achieved only by supporting the cable onto a rigid saddle. This hypothesis will be made, thus eliminating the first effect from the problem.

---

[3] M. Panetti, *I fattori della rigidezza delle funi metalliche* , Atti dalla Reale Accademia delle Scienze di Torino, Cl. di Scienze fisiche, Vol. 79, 1944, pp. 1-37

There is an upper limit on tangential forces since slip may occur once that limit is reached. For a given wire, slip occurs within the cable in the same direction as if it were inextensible.

For a given wire element, slip direction is such that, because of symmetry, wire sections located at extreme positions, that is, inside (concave side) and outside (convex side) of a torus, should not slip.

Tangential force directions are directly related to these displacements, and they act opposite to slip direction.

Besides, tangential forces are made possible because of interwire pressure. Two limit cases are to be considered: either purely radial pressure transmission from one layer to the next; or purely circumferential (lateral) transmission between same layer wires.

In fact, in practical cases, these two modes probably coexist, one of them prevailing over the other, depending on cable geometrical parameters.

However, using one or the other of these limit hypotheses leads to opposite conclusions on tangential force distribution.

Indeed, between two wires belonging to adjacent layers or, more exactly, between the outer and inner layer, their relative slip motion is in the direction away from the neutral axis; thus, the tangential force on the outer wire is directed towards the neutral axis.

As the tensile force increments acting at both ends of the wire element are in opposite directions, tangential forces must decrease further away from the neutral axis, as in solid beams in bending.

If, on the contrary, one considers wires belonging to the same layer, displacement of an element further away from the neutral axis slips with respect to the element closest to the neutral axis in such a way as to get closer to the neutral axis. As in the previous case, a wire element is subjected to a force increment away from the neutral axis. Equilibrium of the element requires that tangential forces will also increase in that direction, which is the opposite of what happens in solid beams in bending.

Slip leads to some wire debonding within the cable. According to hypothesis No 1, debonding occurs from outer to inner layers; and, in a given layer, from wires closest to the neutral axis to those further away, With hypothesis No 2, slip occurs first between wires further away and extends progressively to wires closer to neutral axis.

This process corresponds to a loss in mechanical energy, and, correspondingly, to the work of a friction internal moment. Besides, when debonding is complete, elastic cable resistance to bending is a minimum corresponding to the bending stiffness of wires acting independently.

This work begins with a study of cable geometry. It leads to a relationship between interwire pressure and applied axial load. Here, it is assumed, and is considered as most probable, that contact mode is circumferential rather than radial. The latter assumption has been widely used in earlier works, including by the Author in a paper on the same topic which has been published in 1909 in this Academy's Transactions under the title "*Wire rope elastic modulus under axial load.*"

This contact mode assumption makes it simpler the evaluation of friction work occurring in cable bending, using the limit case of inextensible wires, as well as the calculation of wire tensile forces

resulting from the curvature (called bending forces). Besides, uniform curvature is assumed, which leads to a simple relationship between curvature and bending moment.

This approach makes it possible to separate stiffness modulus evaluation and cable debonding process from the details of cable bending, i.e. from its deformed curve particular geometry, such as the one in Hellmut Ernst's work[4]. Consequently, his results are rather different from those reported in the present paper.

1. Wire geometry

In preparation for the subsequent analysis, the basic equations of a circular helix are recalled. Calling α the lay angle with respect to the cable axis and r the radius of the lay cylinder, helix pitch p, or lay length, is given by:

$$p = 2\pi r \cot\alpha \tag{1}$$

Given α, pitch increases with each layer mean radius.

Going from one layer to the next, with radius increasing, the number of wires increases by 6, while that layer mean radius r increment is practically equal to wire diameter δ. Indeed, perimeters of two adjacent layers mean circles differ by:

$$2\pi(r_2 - r_1) = 2\pi\delta \tag{2}$$

Assuming that on the inner layer, wires are in contact, there will be some gap between those of the outer layer, that gap resulting from the difference between 2π and 6.

However, considering a cable cross-section, wire cross-sections are practically ellipses having a semi-major axis $\delta / \cos\alpha$. Such axis is tangent to the layer mean circle, which goes through wire section center points. Assume now that the mean circle perimeter is practically equal to the circumscribed polygon perimeter; calling z the number of wire in each layer, one gets:

$$2\pi r_1 = z_1\delta / \cos\alpha \qquad\qquad 2\pi r_2 = z_2\delta / \cos\alpha$$

Letting $z_2 - z_1 = 6$, Eq. (2) yields :

$$6 = 2\pi \cos\alpha \tag{3}$$

yielding $\alpha = 17°$ (approximately).

Thus, a lay angle of $17°$ is such that, in a given layer, wires are tightly wound. Such a lay is called "*normal*".

[4] *Beitrag zur Beurteilung der behördlichen Vorschriften für die Seilen von Personenschwebebahnen*, in Fördertechnik und Frachtverkehr, 1933, No 19 to 26 and 1934, No 3 to 7.

When laid at a smaller angle, there will be a gap between outer layer wires. If the angle is larger than $17°$, there should be a gap between layers, which is prevented by wire deformation at points of contact.

It has been shown that helical pitch differs in adjacent layers. This precludes the possibility that outer wires fall in the troughs corresponding to contacting inner wires, even as the outer wires tend to align themselves with the inner ones. Thus, the outer wires will cross over the inner ones like small bridges and, for a constant curvature, they should keep their regular setting.

Frequency of these cross-over is easily derived. Indeed, distance between two same layer neighbouring wires is $\delta / \sin\alpha$ when projected onto cable axis direction. Using Eqs (1) and (2), it is found that this distance is related to the pitch difference between adjacent layers by:

$$(p_2 - p_1) \div \frac{\delta}{\sin\alpha} = 2\pi\cos\alpha$$

From Eq. (3), for a normal lay, there must be 6 cross-over for a complete wire loop. Distance between two cross-over is thus given by :

$$\frac{1}{6}\frac{p}{\cos\alpha}$$

2. *Wire contact conditions*

A strand is made of wires wound helically in concentric layers. A wire rope may be made of one or several strands. Strands may be laid in the same or opposite to wire lay direction. In the first situation, it is a *parallel lay* while in the latter, it is called a *cross lay*. The latter is the most ancient and, even today, it is the one mostly used as it gives a rope better resistance against unwinding. Seen from the outside, a cross lay will show wires almost parallel to the rope axis, while in a parallel lay, wires are clearly at an angle with that axis.

However, in the inter-strand contact region, it is the opposite. This may be shown as follows.

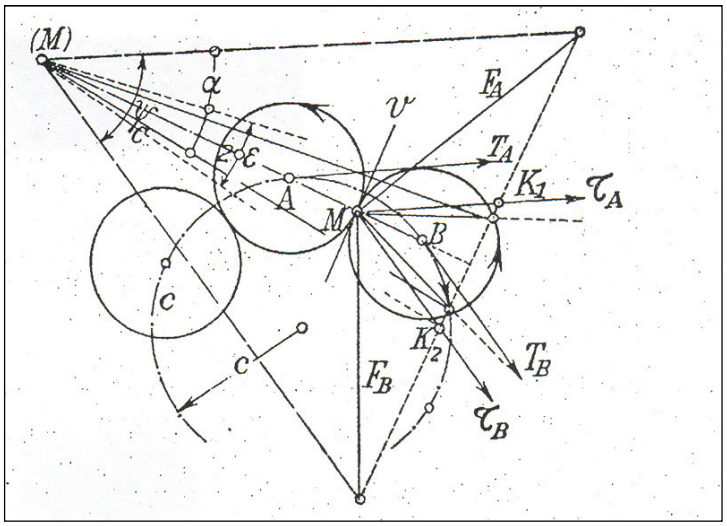

Figure 1

Consider a multi-strand wire rope cross section (Fig. 1). Each strand has been reduced to its corresponding circumscribed circle. It is contacting the adjacent strand at point *M*, at the middle of segment *AB*, *A* and *B* being the circle center points; on each circle, arrows indicate the lay direction, as seen by an observer looking at the given cross-section.

At point *M,* assuming that wire diameter δ is very small, one may consider that contacting wires coincide.

Strand center points are located on circle *c* . Another curved arrow is drawn on that circle, indicating the strand lay direction. Strand lay angle is β, while wire lay angle is α. As already mentioned, lays may be in the same direction or opposite to one another.

In the cross-section neighborhood, strands may be considered to be oblique cylinders with generators parallel to the tangent (*T*) to the corresponding axis. These tangent vectors lie in the plane tangent to the right circular cylinder of radius *c*.

Projection of these tangent vectors onto the plane of the cross-section yields vectors T_A and T_B , tangent to circle *c* at points *A* and *B*. They are in the same direction as the curved arrow on that circle. Parallel lines τ_A and τ_B are drawn at point *M*. They are the projections of generators (τ_A) and(τ_B) from the two contacting cylinders at point *M* .

Let *v* be the line perpendicular to *AB* and to the rope axis. It is coplanar with lines (τ_A) and(τ_B). They make the same angle with respect to the rope cross-section and are symmetrical with respect to the plane which is perpendicular to the cross-section and intersects the latter along *AB*. Hence, the plane containing *v* (τ_A) and(τ_B) is tangent to both skew cylinders contacting at point *M*; thus, tangent lines (F_A) and (F_B) to wires in contact at point *M* must also be in that plane.

Moreover, the angle between lines (*F*) and (τ) is lay angle α, in the direction shown by a curved arrow on each circle *A* and *B*.

In the cross lay case, angle ψ between contacting wires is obtained by adding up angle 2ε between the (τ) lines and angle 2α. In the parallel lay case, angle 2α has to be subtracted.

In order to obtain the true 2ε value, lines (τ_A) and(τ_B) have to be brought onto the figure by rotating around its side K_1K_2 the corresponding isosceles triangle.

From projection K_1MK_2, one obtains the "objective" triangle *K1(M)K2* through the relationship

$$(\mathrm{M})\mathrm{K}_1 = \frac{\mathrm{MK}_1}{\sin\beta}$$

For an n-strand rope, projections of τ lines make an angle $2\pi/\mathrm{n}$ when they intersect at point *M*. From triangle $(M)MK_1$ or its symmetrical, one gets:

$$\sin\varepsilon = \sin\left(\frac{\pi}{\mathrm{n}}\right)\sin\beta \qquad (4)$$

which yields the value for angle ε.

Depending on the type of lay, cross or parallel lay, angle between contacting wires is given by:

$$\psi_c = 2(\varepsilon + \alpha) \qquad \psi_p = 2(\varepsilon - \alpha) \tag{5}$$

For example, for a 6-strand rope, with a 17° lay angle, these equations yield:

$$\frac{\pi}{n} = 30^\circ \quad \varepsilon = 8^\circ - 25' \quad \psi_c = 50^\circ - 50' \quad \psi_p = -(17^\circ - 10')$$

These results show clearly the difference between both types of lay and they also show why parallel lay is preferred when a rope is under cyclic bending.

In fact, the larger angle between contacting wires in cross-lay rope will indeed increase their wear rate.

3. Compact and hollow strands

Strand structure also depends on wire distribution within the cross-section. In the compact case, total number of wires is Z, giving a strand diameter d. Usually, Z is the sum of the base-6 series:

$$z = 6 \quad 2\times 6 \quad 3\times 6 \quad i\times 6$$

and the corresponding radius of each layer is :

$$r = \delta \quad 2\delta \quad 3\delta \quad i\times\delta$$

Last term i is such that :

$$(2i+1)\delta = d \tag{6}$$

Hence :

$$Z = 6(1+2+3+\ldots+\frac{d-\delta}{2\delta}) = \frac{3}{4}\frac{d^2-\delta^2}{\delta^2} \tag{7}$$

Adding up the strand core wire, a very good approximate value for Z is given by:

$$Z = \frac{3}{4}\frac{d^2}{\delta^2} \tag{8}$$

Instead, for a hollow strand, that is, a strand with a textile or hemp core of diameter d_1, wire number Z is given by:

$$Z = \frac{3}{4}\frac{d^2-d_1^2}{\delta^2} \tag{9}$$

Define now an “average” strand radius r_m as follows:

$$Zr_m = z_1 r_1 + z_2 r_2 + z_3 r_3 + \ldots \tag{10}$$

where z_1, z_2 etc. are the number of wires in layers of radius r_1, r_2 etc.

With the above values for z and r, they yield:

$$Zr_m = 6\delta(1 + 4 + 9 + \ldots + i^2) = i(i+1)(2i+1)\delta \tag{11}$$

As for a hollow strand, from Eq. (6):

$$i = \frac{d - \delta}{2\delta} \qquad i_1 = \frac{d_1 - \delta}{2\delta}$$

Hence :

$$i - i_1 = \frac{d - d_1}{2\delta}$$

Finally, using the Z value given either by Eq. (7) (compact strand), or Eq. (9) (hollow strand), the respective average radius value follows:

$$r_m = \frac{d}{3} \qquad r_m^1 = \frac{1}{3}\frac{d^3 - d_1^3}{d^2 - d_1^2} \tag{12}$$

In the second equation, a δ^2.term has been neglected.

4. Strand "self-equilibrium" condition

A basic strand characteristic is the interwire pressure, which results from their helical shape and from the tensile force t acting on each one of them.

An helical wire, curvature $\sin^2\alpha / r$, under tensile force t, must undergo a distributed normal force n, per unit length, given by:

$$n = \frac{t}{r}\sin^2\alpha = t\sin^2\alpha\frac{2\pi}{\delta}\frac{1}{z} \tag{13}$$

In a given layer, consider the product:

$$zn = \frac{2\pi}{\delta} t\sin^2\alpha \tag{14}$$

Assuming the same lay angle, this product is the same for all layers. It is the strand "self-equilibrium" condition.

Two limit cases may be considered regarding the way the normal force n is applied: it may result from lateral contact between same layer wires, or else, it is applied radially, from one layer to the next, down to the core wire.

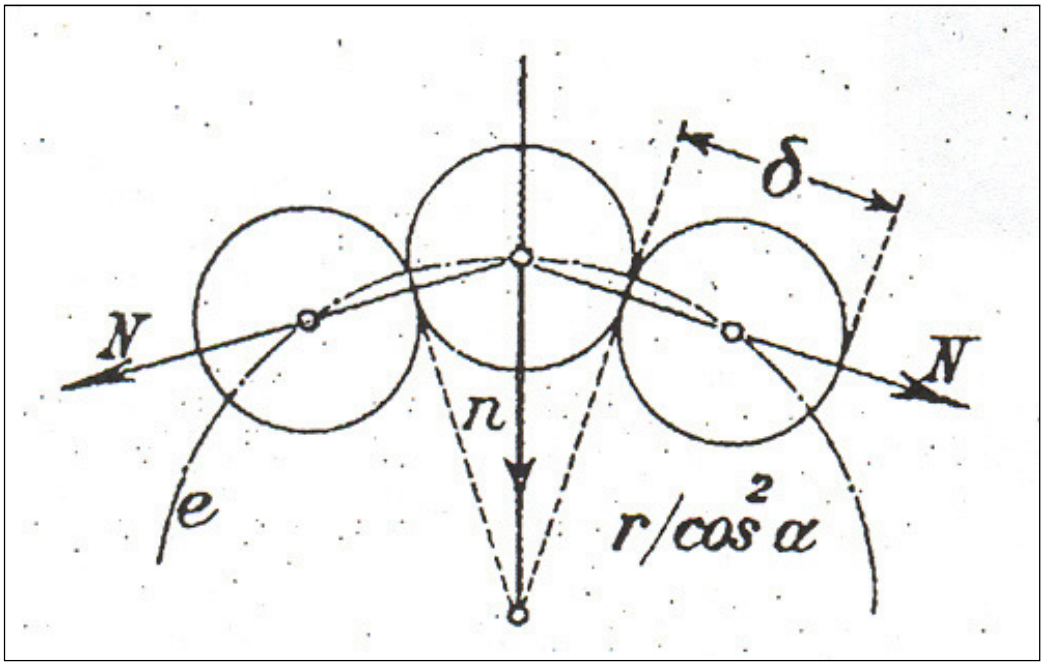

Figure 2

With the first hypothesis, force n is the sum of two normal forces N (Fig. 2), coming from neighboring wires. In that direction, radius of curvature of trajectory *e*, normal to wire axis, is $r / \cos^2 \alpha$. Hence, angle between lines through adjacent wire centers, that is, angle between forces N, is $\delta \cdot \cos^2 \alpha / r$ .This yields :

$$2N \sin\left(\frac{\delta \cdot \cos^2 \alpha}{2r}\right) = n \qquad \text{that is :} \qquad N = t \cdot \frac{\tan^2 \alpha}{\delta} \qquad (15)$$

where it is assumed that the sine value is equivalent to the angle.

Force N is independent of wire location within the strand, and the number of forces N to be considered is equal to the number Z of wires within the strand.

With the second hypothesis, and numbering the layers from the outer one, it will be noticed that, passing from layer 1 to layer 2, one should consider globally the zn forces given by Eq. (14), whose total value, from Eq. (15), is 2πN, that is 6N approximately, letting $\cos \alpha \cong 1$.

Layer 2 is also under a radial pressure equal to 6N to which must be added a pressure exerted on it by layer 1. Thus, total pressure exerted by layer 2 is 12N.

The same approach being used from one layer to the next, radial pressure between layers is given by the following series:

$$\begin{array}{cccccc} 1^{st} \to 2^{nd} & 2^{nd} \to 3^{rd} & 3^{rd} \to 4^{th} & \dots & (i-1)^{th} \to i^{th} \\ 6N & 12N & 18N & & (i-1)6N \end{array}$$

If the innermost layer (number i) is a 6-wire layer wound on a core wire, pressure between layer i and core is iN, as for a 6-wire layer, n and N are equal, since $r = \delta$.

Total is still ZN. Indeed, $6(1+2+3+\dots+i) = 3i(i+1) = Z$, total number of wires in strand. However, one gets the same result, even if the calculation stops at any inner layer i . Such layer comprises $Z - 6(i-1)$ wires. It is acted on by radial load $i \times n$ and, according to Eq. (15), this is transformed to $i \times N$ through tangential forces from the last layer.

In fact, taking the sum yields:

$$6N\left[1+2+3+\dots+(i-1)\right]+\left[Z-6(i-1)\right]iN = \left[iZ-3i(i-1)\right]N$$

where force N is still multiplied by total number Z.

Hence, taking either hypothesis, radial or lateral wire contact, total pressure between wires in a strand is given by the same value ZN.

In practice, pressure transmission will follow an intermediate pattern, between radial and lateral, depending on the degree of compactness of same layer wires. This depends on the layer lay angle: an angle greater than the normal angle leading to more lateral contact, while a lay angle smaller than the normal angle leads to more radial contact.

In fact, contact forces determination is a statically undetermined problem. A solution would require calculation of contact deformations, assuming elastic behaviour; because interlayer contacts are point contacts (Section 1) radial compliance is obviously greater than lateral compliance. It is thus logical to assume that lateral contact is the prevailing mode.

This contact mode is such that outer layer wires are locked in place which is advantageous in the case of a wire break.

Besides, in the radial contact mode, wires are subjected to bending between supporting contact points (distance between neighboring contacts has already been given), thus increasing metal fatigue problems.

It will be assumed that, even for a mixed contact mode, resultant of internal forces is the same as the one found in the limit cases. Hence:

$$ZN = Zt\frac{\tan^2\alpha}{\delta} = \frac{T}{\cos\alpha}\frac{\tan^2\alpha}{\delta} \qquad (16)$$

in which T is the total traction force on the cable. This so-called “self-locking” condition depends directly on T through a constant factor. Assuming that $\cos\alpha \cong 1$, this factor is practically $\sin^2\alpha/\delta$, as with a single wire.

However, even if the self-locking condition is the same, the contact mode, either lateral or radial, is not without consequence on bending stiffness. This is shown in the sequel.

Actually, in the lateral mode, contact pressure is uniformly distributed within the cross-section, while in the radial mode, they add up when getting closer to the core.

Thus, a larger bending stiffness is to be expected in the lateral mode.

Finally, consider the self-locking effect due to the cable helical strand laying. Here, one has only one layer, without a core. In Eq. (15), the second equation still applies, with the following substitutions: T instead of t; β instead of α; and d instead of δ. Thus, the force per unit length between strands is given by:

$$H = T\frac{\tan^2 \beta}{d} \tag{17}$$

That force will be transmitted to individual wires, taking into account their angle ψ (Section 2).

5. Bending induced slip within a strand

Assume now that a rectilinear strand is given a uniform curvature R, taking a circular shape. First, it is assumed that its axial length is kept constant and also that plane cross-sections remain plane; however, as the strand passes from a cylindrical to a toroidal shape, individual wires have to slip, keeping the same length, as if inextensible.

Such system is of course theoretical, defined purely in geometrical terms, without material properties, while at the same time deformable. Such model is useful to study wire slip and, first of all, to show that the assumed wire inextensibility is compatible with the assumed deformation.

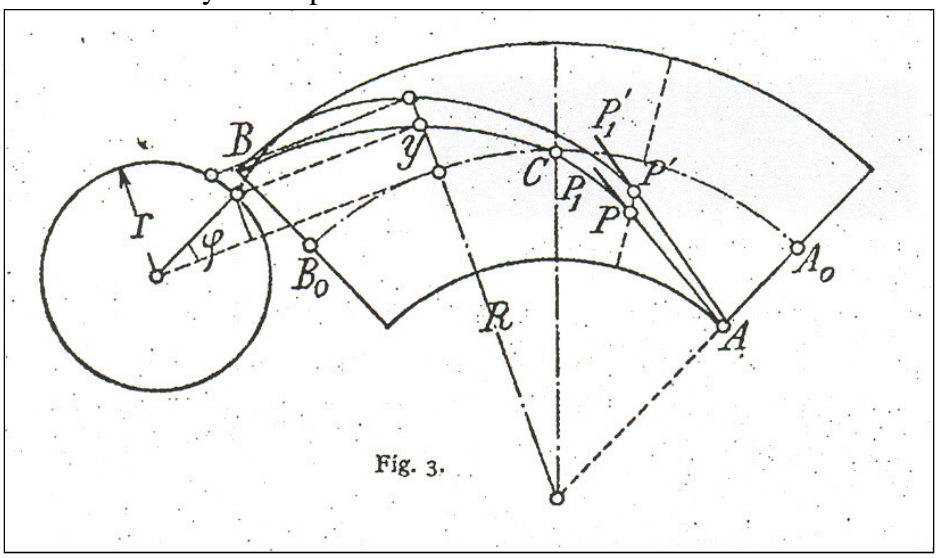

Figure 3

Such deformation has the same geometrical characteristics as in the pure bending of a cylindrical elastic solid: i.e. there is a neutral layer, of radius R, boundary between two regions of the solid, one

being in tension and the other in compression. Stresses are obtained from the strains: in a given cross-section, a point at a distance y from the neutral layer is under a strain y/R (Fig. 3).

Before deformation, a wire on cylinder of radius r is defined by the circular helix equation:

$$\frac{x}{p} = \frac{\varphi}{2\pi} \qquad y = r\sin\varphi \tag{18}$$

In this equation, coordinate x is measured on the strand axis and its origin corresponds to $\varphi = 0$ on the given wire. It is the point *C* at which wire axis intersects a plane which will become, after bending, the neutral layer of this fictitious body.

Helix element $d\ell$ taken on a given wire centerline is given by:

$$d\ell = \frac{dx}{\cos\alpha} = \frac{p}{2\pi\cos\alpha}d\varphi = \frac{r}{\sin\alpha}d\varphi \tag{19}$$

After bending, it undergoes an elongation which may be derived from the axial element dx, which is $\frac{y}{R}dx$. Its projection onto direction ℓ is

$$\Delta(d\ell) = dx\frac{y}{R}\cos\alpha = \frac{r}{R}\sin\varphi\frac{p}{2\pi}\cos\alpha d\varphi = \frac{r^2}{R}\sin\varphi\frac{\cos^2\alpha}{\sin\alpha}d\varphi \tag{20}$$

Consider a strand element between two cross-sections whose distance is half the lay length p. It is bounded by cross-section A_0 corresponding to x = -p/4 and $\varphi = -\pi/2$, and cross-section B_0 corresponding to x = +p/4 and $\varphi = +\pi/2$. There must be no length variation of half-loop *ACB* (Fig.3).

Indeed, it is obvious that integration of Eq. (20) on this interval does vanish.

Hence, length of deformed curve *ACB* is equal to that of the corresponding helix half-loop. Arc *AC* contracts, while arc *CB* stretches, assuming that *B* is on the torus convex side and *A* on the concave side. It is thus possible that end points *A* and *B* of the inextensible wire which corresponds to the half-loop stay in place (do not move) while any other point *P* of the half-loop will slip with respect to the rest of the strand.

Thus, if *P* is located on arc *AC*, on the compression side, the corresponding theoretical fiber is shortened and the end *P* of arc *AP* sticks out of the normal cross-section by an amount PP_1 which is equal and opposite to variation $\Delta(d\ell)$, that quantity being calculated from *A* to *P*.

Local slip of wire with respect to the rest of the strand is:

$$s = -\int_A^P \Delta(d\ell) = -\frac{r^2\cos^2\alpha}{R\sin\alpha}\int_{-\pi/2}^{\varphi}\sin\varphi d\varphi = \frac{r^2}{R}\frac{\cos^2\alpha}{\sin\alpha}\cos\varphi \tag{21}$$

Such slip is a function of φ and r. Its maximum value is reached for $\varphi = 0$. That value is given by:

$$S = \frac{r^2}{R}\frac{\cos^2\alpha}{\sin\alpha} \tag{21'}$$

Work of friction forces, which result from inter-wire pressure, does not depend on displacement s but, rather, on its relative value (s) for the contacting wires.

For same layer wires, calculation of (s) depends on parameter φ. Indeed, passing from one wire to the next, for a given abscissa x, the corresponding jump on angle φ is:

$$\Delta\varphi = \frac{\delta}{r}\cos\alpha$$

Displacement variation is obtained by multiplying $\Delta\varphi$ by $\frac{\partial s}{\partial\varphi}$. Yielding:

$$(s)_1 = -\frac{r}{R}\cot\alpha\cos^2\alpha\ \ \delta\sin\varphi \tag{22}$$

It can be seen on Fig. 3 that relative displacement $(s)_1$ results from the fact that points *P* and *P'*, which correspond to wire centerline intersecting with given strand cross-section, undergo slip amplitudes s which are PP_1 and $P'P_1'$ respectively. Such slip amplitudes are not equal because distance of *P* and *P'* from the corresponding wire fixed point is different.

Now, if contacting wires belong to adjacent layers, consider contacting elements that is, those which correspond for a given strand curvature. For such elements, angle φ is the same. However, their radius r differs by an increment δ. Relative slip between wires is given by:

$$(s)_2 = 2\frac{r}{R}\frac{\cos^2\alpha}{\sin\alpha}\delta\cos\varphi \tag{23}$$

In this case, relative slip is a cosine function of φ. There is a 90° phase lag between $(s)_1$ (same layer contact) and $(s)_2$ (inter-layer contact). Noting that cosα is close to unity, amplitude of the latter is approximately twice that of the former.

Friction between contacting wires tends to decrease slip. Indeed, as strand curvature increases, wire stress increase corresponds to elastic strain, thus leading to slip decrease.

Such effect is small and, at this stage, it will be neglected.

6. Friction work

Friction work is a result of friction forces arising from contact pressure (determined in Section 4) doing work because of slip displacements.

Friction forces $fNd\ell$ correspond to displacements $(s)_1$; friction forces $fnd\ell$ correspond to displacements $(s)_2$. Recall that N and n are lateral and radial pressures, respectively.

Along a given wire or, better, for same layer wires, both of these pressures take on a constant value, while displacements (s) show a periodic variation. Elementary works are:

$$fN(s)_1 d\ell \qquad fn(s)_2 d\ell \tag{24}$$

Their average value over a period, that is a lay length, may be obtained.

However, as friction work is always negative, integration interval may be taken as p/4, where φ varies from zero to π/2.

Thus, average friction works are:

$$X_1 = \frac{4}{p}\int_0^{\pi/2} fN(s)_1 d\ell \qquad X_2 = \frac{4}{p}\int_0^{\pi/2} fn(s)_2 d\ell \tag{25}$$

corresponding respectively to lateral pressure between same layer wires and radial pressure between adjacent layer wires.

Works X_1 and X_2 are works per unit wire length in projection onto strand axis, corresponding to friction forces projected onto strand axis. Hence, they should be multiplied by the length of the strand segment which passes from the rectilinear state to the curved one. However, as these are mean values taken over a period, calculation should be made taking a strand length being a multiple of lay length.

But, taking the sum over all wires in the strand:

$$\mathfrak{X}_1 = \sum X_1 \qquad \mathfrak{X}_2 = \sum X_2 \tag{26}$$

one gets the same result as the one obtained summing elementary work (24) over all wires in an elementary strand segment, and then dividing by dx; indeed, taking the entire set of wire elements at a given cross-section, one has the values of the periodic function whose mean value is being calculated.

Thus, the $\mathfrak{X}$ are equivalent friction forces reduced to the strand axis. They may be considered as a strand anelastic stiffness. Similarly,

$$M_w = \mathfrak{X} R$$

is the corresponding reduced moment. Assuming a relative rotation $d\varphi = \frac{dx}{R}$ of the strand element bounding faces, work of M_w in that rotation is the same as the corresponding reduced force work $\mathfrak{X} dx$.

Reduced forces $\mathfrak{X}$ are determined from Eqs (25), substituting functions n, N, $(s)_1$, $(s)_2$, $d\ell$ with corresponding values obtained from Eqs (13), (15), (22), (23) and (19).

For each of the contact hypotheses, lateral and radial, friction work is:

$$X_1 = \frac{2}{\pi} ft \frac{\sin\alpha}{\cos^2\alpha} \frac{1}{R} \qquad X_2 = \frac{4}{\pi} ft \sin\alpha \cos\alpha \frac{\delta}{R}$$

One can see that X_1 is a function of curvature, while X_2 is independent of that quantity (?)

Multiplying X_2 by the number of wires, and letting $T = Zt\cos\alpha$, it yields :

$$\mathfrak{X}_2 = \frac{4}{\pi} fT \sin\alpha \frac{\delta}{R} = \frac{M_{w2}}{R} \tag{27}$$

In order to get $\mathfrak{X}_1$, sum must be performed layer per layer. Using the average radius r_m given by Eq. (10), one gets:

$$\mathfrak{X}_1 = \frac{2}{\pi} fT \frac{\sin\alpha}{\cos^3\alpha} \frac{r_m}{R} = \frac{M_{w1}}{R} \tag{28}$$

Both anelastic stiffnesses $\mathfrak{X}_1$ and $\mathfrak{X}_2$ are of the same order of magnitude in the case of compact structures, which corresponds to the first of Eqs (12), with $d = 6\delta$, that is for intermediate structures, between 18 and 36 wires.

In textile core strands, which are generally made of two layers, radial contact is possible between these layers only and the inner layer must undergo the lateral contact mode. The corresponding anelastic stiffness given by Eq. (28) may be used in which the average radius is taken as:

$$r_m = \frac{1}{2}(d - 2\delta)$$

7. Multistrand cable stiffness

Consider an n-strand cable in bending, radius of curvature R. Each strand initial curvature is $\sin^2\beta / c$. After bending, it becomes $1/\rho$, varying from one point to the other. It may be estimated, assuming that the strand axis intersects the great circles on the torus surface under a constant winding angle β (Fig.4).

Consider points *E* and *J*, at which strand axis intersects the external circle *(e),* radius R+c (convex side) and internal circle *(j),* radius R-c (concave side), on the toroidal surface. Corresponding curvatures are:

$$\frac{1}{\rho_E} = \frac{\cos^2\beta}{R + c} + \frac{\sin^2\beta}{c}$$

$$\frac{1}{\rho_J} = \frac{\cos^2\beta}{R - c} - \frac{\sin^2\beta}{c}$$

Subtracting the initial curvature $\pm\sin^2\beta / c$, one gets the local curvature increase:

$$\frac{\cos^2\beta}{R + c} \quad \text{and} \quad \frac{\cos^2\beta}{R - c}$$

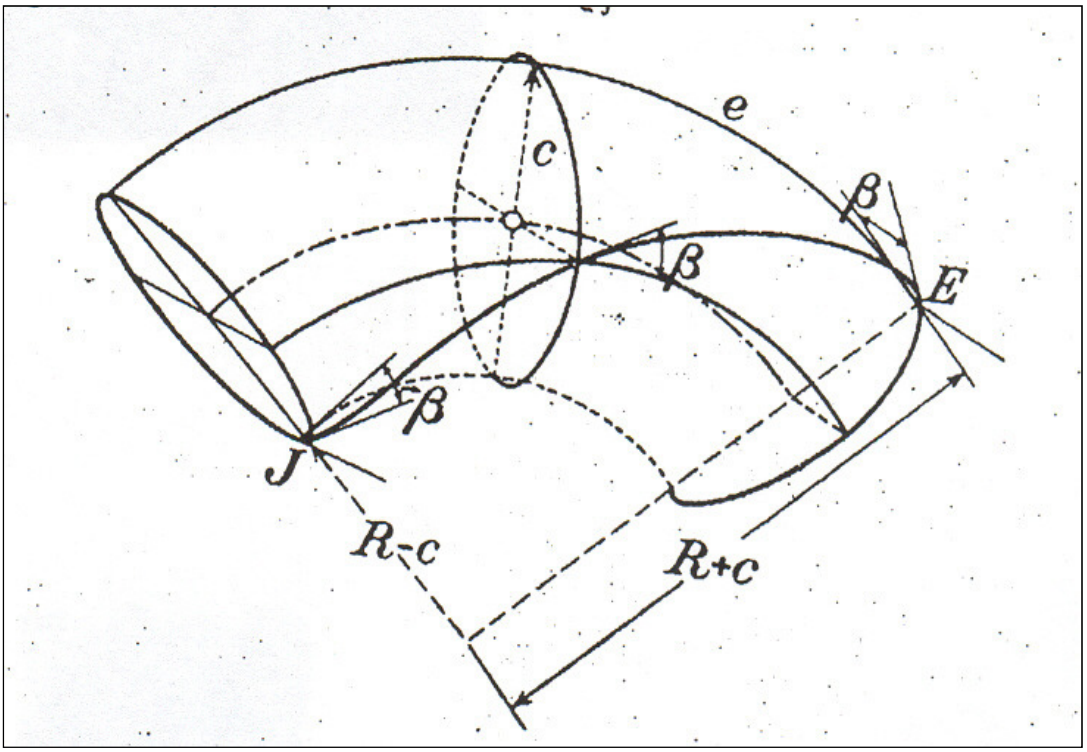

Figure 4

The mean of these extreme values is $\cos^2\beta / R$. It will be taken as the approximate value of the strand axis curvature, instead of 1/R.

Cable bending stiffness, which is the sum of the strand stiffness, is obtained multiplying Eq. (28) by n, and replacing 1/R by $\cos^2\beta / R$.

Total axial force on cable is given by:

$$\mathfrak{T} = nT\cos\beta$$

Thus :

$$\sum \mathfrak{X} = \frac{2}{\pi} f\mathfrak{T} \frac{\sin\alpha}{\cos^3\alpha\cos\beta} \frac{r_m}{R} \tag{29}$$

where, again, r_m is the average strand radius.

However, inter-strand friction also contributes because of pressure H. It is determined with Eq. (17) and slip is obtained from Eq. (22), where strand geometric parameters have to be substituted to those of wires; hence parameters c, d, β have to replace r, δ et α. Thus, elementary work performed on the corresponding slip is:

$$f_1 H \frac{c}{R} \frac{d}{\sin\beta\cos\beta} \sin\varphi \frac{c}{\sin\beta} d\varphi$$

This yields the average value for a given strand :

$$\frac{2}{\pi} f_1 T \frac{c}{R} \frac{\sin\beta}{\cos^2\beta}$$

This value, multiplied by the number of strands n has to be added to Eq. (29).

Thus, cable stiffness is given by:

$$(\mathfrak{X}) = \frac{2\mathfrak{T}}{\pi R}\left(fr_m \frac{\sin\alpha}{\cos^3\alpha\cos\beta} + f_1 c \frac{\sin\beta}{\cos^3\beta} \right) \tag{30}$$

Inter-strand friction coefficient f_1 may be different from inter-wire coefficient f. This because of the differing contacting surfaces, but also, it will depend on angle ψ between wires of adjacent strands, which itself depends on the type of cable lay, parallel or cross lay (Section 2).

8. Bending tensile forces

It has been assumed that slip due to bending was a result of wire inextensibility. This hypothesis is not sufficient to explain the actual cable behavior. It is indeed more logical to assume that, as curvature is increased, wire tensile forces increase up to a point at which friction force reaches a limit value. At that point, there is impending slip.

These tension increments, noted Δt, which differ in each wire, will be called *bending tensions*.

In the classical solid beam theory, bending tensions are parallel to the beam axis. If beam curvature and tension are given, these bending tensions are constant.

Thus, for a solid prismatic beam, it is only in the case of a variable curvature that internal equilibrium requires non-zero forces parallel to beam axis between parallel layers.

In a strand, on the contrary, bending tensions are parallel to each wire axis. Even when curvature is uniform, they vary along each wire from one point to the other. They depend on distance y from neutral axis, which itself is a function of angle φ.

Hence, there must be a tangential force V acting on a wire surface.

It is assumed that Δt is a force acting on a square cross-section, δ by δ, within which the round wire section is inscribed.
In the same fashion, tangential force V is assumed to act on a band, width δ, length δ.

Hence, a given wire is acted upon by a tangential force per unit length V/δ.

Assuming that lateral mode of contact prevails, limit value on force V is given by:

$$\frac{V}{\delta} \leq fN \tag{31}$$

where N is given by Eq. (15) . It is a force per unit length and it corresponds to a band, width δ, as defined for each wire.

As with slip displacements in Section 5, with uniform strand curvature, it is logical to assume that bending tension Δt, as well as tangential force V, take the same value for a given distance y from the neutral axis. That is, for any wire, they will depend only on $r \sin \varphi$.

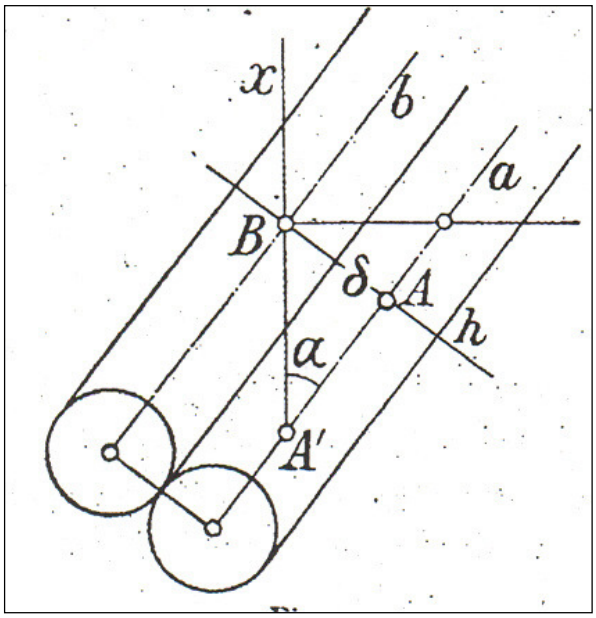

Figure 5

Consider two same-layer adjacent wires (Fig. 5). Their respective axes *a* and *b* are at a distance *δ* and make an angle *α* with respect to strand axis. Take points *A'* and *B* on a straight line parallel to direction *x*. Bending forces Δt on corresponding sections must take the same value.

Consider now transverse direction *h*, from *B* to *A*, taken, as point *A'*, on axis *a*. Bending force Δt must vary in the same fashion, going either from *A* to *A'*, or from *A* to *B*.

This condition yields:

$$\frac{\partial(\Delta t)}{\partial \ell} AA' = \frac{\partial(\Delta t)}{\partial h} \delta \tag{32}$$

where :

$$\delta = AA' \tan \alpha \tag{33}$$

Besides, equilibrium of wire element $d\ell$ requires that tension variation Δt has to be balanced by the differential on tangential force $V d\ell / \delta$ acting on its side, which is:

$$\frac{\partial}{\partial h}\left(V \frac{d\ell}{\delta} \right) dh$$

Noting that $dh = \delta$, such differential becomes: $\frac{\partial V}{\partial h} d\ell$

Thus, the equilibrium condition yields:

$$\frac{\partial(\Delta t)}{\partial \ell} + \frac{\partial V}{\partial h} = 0 \tag{34}$$

Using Eqs (32) and (33), it yields :

$$\frac{\partial(\Delta t)}{\partial h} \tan\alpha + \frac{\partial V}{\partial h} = 0 \tag{35}$$

Thus :

$$\Delta t \tan\alpha + V = cst$$

However, near the section neutral axis, $\Delta t = 0$, and relative slip $(s)_1$ between adjacent same layer wires also vanishes, as seen from Eq. (22), Thus the integration constant in the above equation must vanish. Hence:

$$V = -\Delta t \tan\alpha \tag{36}$$

This implies that, on the strand cross-section, axial and tangential bending forces are proportional. Compared to the solid beam case, this is a distinctly different behaviour.

In boundary condition Eq. (31), V is a strictly positive quantity. Force N being given by Eq. (15) and letting:

$$t = t_0 \pm \Delta t$$

limit value $(\Delta t)_0$ of bending forces due to friction is:

$$\mp(\Delta t)_0 = \frac{t_0 f \tan\alpha}{1 \pm f \tan\alpha} \tag{37}$$

In Eq. (37), the upper sign applies in the compression side, where $t < t_0$; slip limit is smaller, and slip will initiate in that region. The lower sign applies in the tension side.

9. Strain and slip

It is first assumed that wires behave as in a solid beam, and that the plane cross-section hypothesis is valid. Stretch of wire element $d\ell$, on layer of radius r, is given by Eq. (20).

Corresponding strain is:

$$\varepsilon = \frac{\Delta(d\ell)}{d\ell} = \frac{y}{R}\cos^2\alpha \tag{38}$$

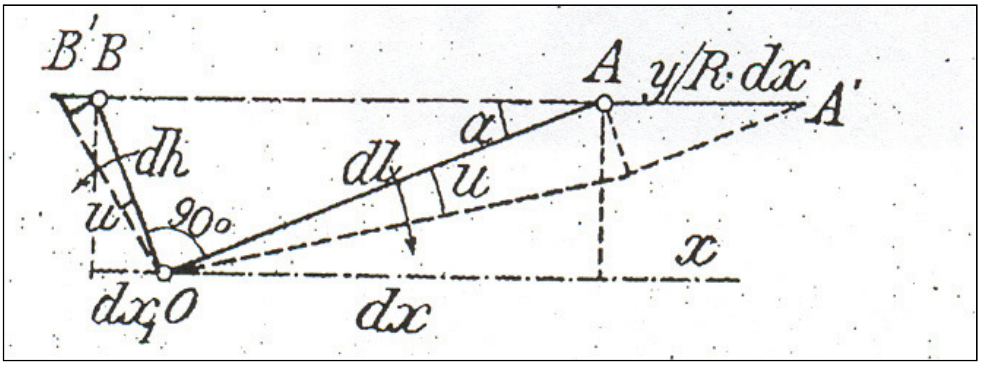

Figure 6

Also, displacement in direction x of the end point A of element $OA = d\ell$ is $dx\frac{y}{R}$. Taking its projection onto the normal direction to ℓ and dividing by $d\ell$ (Fig. 6), one gets the rotation u of element $d\ell$:

$$\frac{dx(y/R)\sin\alpha}{dx/\cos\alpha} = \frac{y}{R}\sin\alpha\cos\alpha \tag{39}$$

This is of course assuming that transverse contraction of strand resulting from axial strain is neglected.

In a direction normal to wire axis, and in plane tangent to cylinder of radius r, line element $dh = OB$ projects onto strand axis as $dx_1 = dh\sin\alpha$. Displacement of point B with respect to O has a component parallel to the x direction :

$$BB' = \frac{y}{R}dx_1$$

Projection of *BB'* onto the normal direction to h, divided by dh, yields its angle of rotation and it is equal, in absolute value and opposite direction, to Eq. (39).

Shear strain is the algebraic difference between the two rotations, and is equal to twice Eq. (38), that is

$$\gamma = -2\sin\alpha\cos\alpha\frac{y}{R} \tag{40}$$

It is negative when $y > 0$, as the angle between initially orthogonal elements $d\ell$ and dh is now larger than 90°.

Letting a be the wire cross-section, relationship between bending forces Δt, tangential forces V, and corresponding strains are:

$$\Delta t = Ea\varepsilon = Ea\frac{y}{R}\cos^2\alpha$$
$$V = KEa\gamma = -2KEa\sin\alpha\cos\alpha\frac{y}{R} \qquad (41)$$

where K is a factor such that, when multiplied by the wire axial elastic modulus, one gets the ratio between tangential forces and shear strain.

Combining Eqs. (40), (41) and Eq. (36) found in the preceding section from the condition of internal equilibrium, yields

$$K = \frac{1}{2}$$

Correlation factor between tangential force and strain appears to be independent on strand internal structure. According to this approach, it is obtained arbitrarily from an equivalent solid body.

10. A direct calculation of factor K

Another approach is tried, based on the following remark. Assume that tangential force per unit length V/δ , acting parallel to wire generator *g* , is uniformly distributed over chord 2c, drawn at distance *h* from center of circular section, radius δ/2 (Fig. 7).

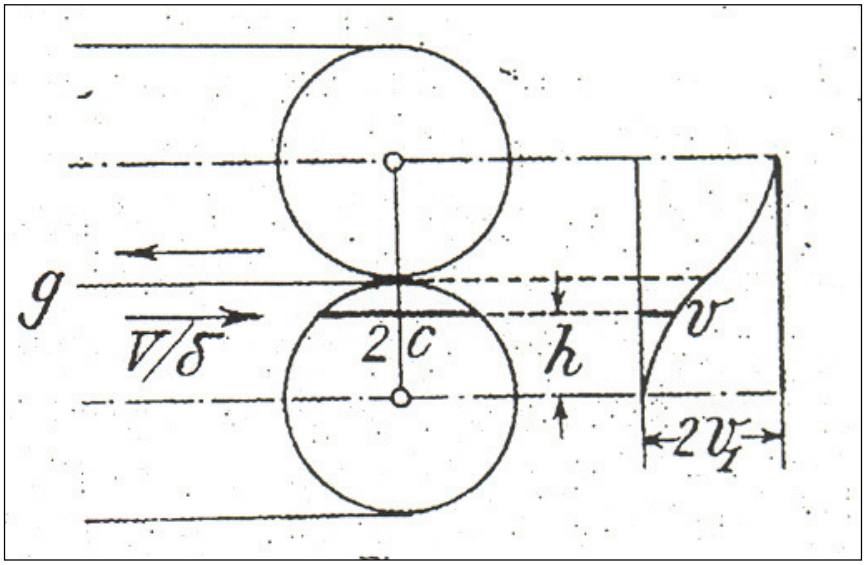

Figure 7

Distributed tangential force is

$$\tau = \frac{V}{2c\delta} = \frac{KEa\gamma}{2\delta\sqrt{\frac{\delta^2}{4} - h^2}}$$

It acts on the circular section chords, starting from that point at which the given wire is in contact with adjacent wire, up to the diameter normal to the loading plane. It corresponds to warping of wire cross-section.

Consider the radial line, belonging to the loading plane, along which distance h is measured. It undergoes a displacement v such that, at any point:

$$\frac{dv}{dh} = \frac{\tau}{G} = \frac{\pi}{4}\gamma K \frac{E}{G}\left(1 - \frac{4h^2}{\delta^2}\right)^{-\frac{1}{2}}$$

Integrating from h = 0 to h = δ/2, one gets the displacement at the contact point:

$$v_1 = \frac{\pi^2}{16}\gamma K \frac{E}{G}\delta \tag{42}$$

Relative displacement of corresponding points on same layer adjacent wires is twice this value.

Letting $\frac{2v_1}{\delta} = \gamma$, this yields

$$K = \frac{8}{\pi^2}\frac{G}{E} \tag{43}$$

Using typical values for the ratio of elastic moduli ratio, this yields a factor K of about 1/3.

Whatever the validity of this approach, as well as the interpretation that can be given to the diverging K values of 1/2 , given by Eq. (41), and 1/3 found above, it looks obvious that the plane section hypothesis (that a strand plane cross-section remains plane after bending), does not yield enough parameters in order to satisfy system deformation conditions.

11. Bending forces taking into account cross-section warping

Thanks to Prof. Placido Cicala's kind suggestion, it can be shown that a more general approach of this problem can be obtained by dropping the plane section hypothesis. This means that a point on a wire axis is allowed to undergo a displacement u with respect to the strand cross-section on which it is located before bending, without loss of solidarity between wires in contact. Such displacement u is a function of parameters φ and r only.

Function u has the same geometrical properties as slip s found in Section 5, where wires were supposed to be inextensible; here, however, it is a displacement arising from wire elasticity.

Variation of element $d\ell$ elastic elongation arising from displacement u is given by

$$\frac{\partial u}{\partial \ell} d\ell \tag{44}$$

Dividing by $d\ell$ yields its value per unit length. It provides a term to be added to the expression for strain ε found in Eq. (38):

$$\frac{\partial u}{\partial \ell} = \frac{\partial u}{\partial \varphi}\frac{\partial \varphi}{\partial \ell} = \frac{\partial u}{\partial \varphi}\frac{\sin\alpha}{r} \tag{45}$$

Similarly (Fig. 5), consider a displacement in direction *h*, perpendicular to wire axis on a given layer. For shear strain γ, the corresponding term to be added to the one given by Eq. (40) is

$$\frac{\partial u}{\partial h} = \frac{\partial u}{\partial \varphi}\frac{\partial \varphi}{\partial h} = \frac{\partial u}{\partial \varphi}\frac{1}{r\cos\alpha} \tag{46}$$

With $y = r\sin\varphi$, normal and tangential bending forces are given by

$$\begin{aligned} \Delta t &= Ea\left(\frac{r}{R}\cos^2\alpha\sin\varphi + \frac{\partial u}{\partial \varphi}\frac{\sin\alpha}{r}\right) \\ V &= KEa\left(\frac{\partial u}{\partial \varphi}\frac{1}{r\cos\alpha} - 2\frac{r}{R}\sin\alpha\cos\alpha\sin\varphi\right) \end{aligned} \tag{47}$$

Using Eq. (36), these equations yield :

$$\frac{\partial u}{\partial \varphi}(K + \sin^2\alpha) = \frac{r^2}{R}\sin\alpha\cos^2\alpha(2K-1)\sin\varphi \tag{48}$$

Integration with respect to variable φ yields :

$$\begin{aligned} u &= k\frac{r^2}{R}\cos\varphi \\ \text{with} \quad k &= \frac{\sin\alpha\cos^2\alpha(1-2K)}{K+\sin^2\alpha} \end{aligned} \tag{49}$$

As previously, the hypothesis according to which function u, as does function s, vanishes at the upper and lower points of a given wire loop, has been taken into account in the integration.

Eq. (48) does not impose a specific value on parameter K. However, it leads to new equations for the bending forces:

$$\Delta t = Ea(\cos^2\alpha - k\sin\alpha)\frac{y}{R} = \xi Ea\frac{y}{R} \quad \text{with :}$$
$$\xi = \frac{1+2\sin^2\alpha}{K+\sin^2\alpha} K\cos^2\alpha \tag{50}$$

If, for example : K = 1/3 and $\alpha = 17°$,

It yields : k = 0.213 and $\xi = 0.85$

while the plane section hypothesis yields $\xi = 0.914$.

12. Bending tension diagram

In both cases, Eqs (41) and (50) only apply as long as tangential force is not greater than friction limit, i.e. as long as Eq. (31) holds. Thus, they apply as long as bending tensions are smaller than limit value $(\Delta t)_0$ given by Eq. (37).

Ordinates of a wire stick and slip regions boundary points are given by:

$$\frac{y_1}{R} = \frac{t_0}{Ea}\frac{f\tan\alpha}{\xi(1-f\tan\alpha)} \qquad -\frac{y_2}{R} = \frac{t_0}{Ea}\frac{f\tan\alpha}{\xi(1+f\tan\alpha)} \tag{51}$$

Letting for example f = 0.15 and $Ea = 500t_0$:

$$\frac{y_1}{R} = 1.15\times10^{-4} \qquad -\frac{y_2}{R} = 1.05\times10^{-4}$$

yielding an average value of 1.1×10^{-4}.

Outside the slip region, (Δt) keeps its constant value $(\Delta t)_0$, and its variation can be shown as in Fig. (8).

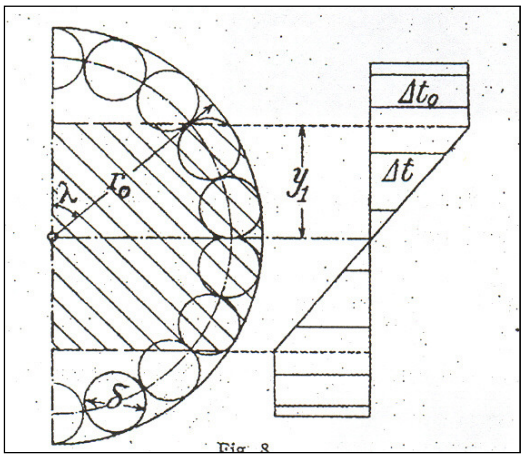

Figure 8

In Eq. (51) denominator, neglecting $f\tan\alpha$ compared to unity, y_1 and y_2 absolute values, as well as that of $(\Delta t)_0$ in Eq. (37), simplify to:

$$\frac{y_1}{R} = f\,\frac{\tan\alpha}{\xi}\,\frac{t_0}{Ea} \qquad (\Delta t)_0 = f\,\tan\alpha\,t_0 \tag{52}$$

Thus, as strand curvature increases (or else, as radius of curvature R decreases), wire stick zone, of amplitude $2y_1$, decreases.

In practical cable machines, it is possible to consider that, at cable/pulley contact, R ≤50d, yielding:

$$\frac{y_1}{d} \le 0.0055$$

which means that the stick zone extends above and below the neutral axis at a distance smaller than 1/100 of strand diameter d.

Thus, one may assume that $(\Delta t)_0$ applies over the whole section, with a plus sign in the extension and a minus sign in the compression region.

The absolute value of the corresponding elastic strain is:

$$\frac{(\Delta t)_0}{Ea} = \frac{f\,\tan\alpha\,t_0}{Ea}$$

It corresponds to a slip s' which has to be subtracted from slip s obtained with the inextensible wire hypothesis.

Recalling that the upper (convex side) and lower (concave side) sections of a wire undergo no displacement, one gets:

$$s' = f\,\frac{\tan\alpha\cdot t_0}{Ea}\,\ell$$

where ℓ is a wire length measured from the closest fixed section.

Maximum value of s' is noted S' occurring at section neutral axis. At that point, $\ell = \pi r/2\sin\alpha$ (a quarter of a wire loop). Hence:

$$S' = f\,\frac{\pi r}{2\cos\alpha}\,\frac{t_0}{Ea}$$

which increases with ratio t_0/Ea.

On the contrary, from Eq. (21'), maximum S of slip function s increases with ratio r/R. Taking the usual values for f and α, both displacements may be compared:

$$S'\Big/\frac{t_0}{Ea} = 0.245r \qquad S\Big/\frac{r}{R} = 3.13r$$

With the selected conditions, S' is quite small compared with S. This confirms the validity of the inextensible wire hypothesis, used in Section 6, where only slip s was used in the friction work computation.

13. Reacting bending moments

Reacting elastic bending moment has two components:

1. A component arising from wire bending stiffness acting independently. For a simple strand, it is given by the equation:

$$M_1 = ZEa\left(\frac{\delta}{4}\right)^2 \frac{\cos^3 \alpha}{R} \tag{53}$$

Indeed, $\cos^2 \alpha / R$ is the average wire curvature increase. Besides, individual wire bending moments are vectors making an angle α with the resulting moment. It is the sum of their projections onto the strand cross-section.

2. A component arising from bending tensions. Within the stick region, they are proportional to distance from neutral axis. In the slip region, they have the constant value $(\Delta t)_0$.

Hence, using Eqs (50) and (52):

$$M_2 = 2\xi \frac{Ea}{R} \sum_0^{y_1} y^2 + 2f \tan \alpha \; t_0 \sum_{y_1}^{y'} y \tag{54}$$

where y' is the ordinate of wire section center most distant from neutral axis.

In Eq. (54), discrete sums Σ can be replaced by integrals over the strand cross-section.

This is done by multiplying and dividing by $\delta^2 = dx.dy$, as in the summation, each wire is replaced by a circumscribed square.

Thus, assuming a strand compact structure:

$$\sum y^2 = \frac{1}{\delta^2} \int \int y^2 dx dy = \frac{2}{\delta^2} \int \sqrt{r^2 - y^2}\, y^2 dy$$

in which the x integration has been performed over a cord of circle, radius r. Then, a second integration must be performed:

$$\int \sqrt{r^2 - y^2}\, y^2 dy = -\frac{1}{8} y(r^2 - 2y^2)\sqrt{r^2 - y^2} - \frac{r^4}{16} \sin^{-1} \frac{(r^2 - 2y^2)}{r^2}$$

At the lower boundary y=0, this expression yields $-\frac{\pi r^4}{32}$. Thus, in Eq. (54), first term becomes:

$$M_2' = \frac{\xi Ea}{2R\delta^2}\left[\frac{r_0^4}{2}\cos^{-1}\frac{r_0^2 - 2y_1^2}{r_0^2} - y_1\left(r_0^2 - 2y_1^2\right)\sqrt{r_0^2 - y_1^2}\right]$$

Letting $y_1 = r_0 \cos\lambda$, it yields :

$$M_2' = \frac{\pi}{16}\frac{\xi E r_0^4}{R}\left[\pi - 2\lambda + \frac{\sin 4\lambda}{2}\right] \tag{55}$$

where $r_0 = d/2$ is radius of strand circumscribed circle.

Similarly:

$$\sum y = \frac{1}{\delta^2}\int y\,dx\,dy = \frac{1}{\delta^2}\int \sqrt{r^2 - y^2}\,dy^2 = -\frac{2}{3\delta^2}\left(r^2 - y^2\right)^{3/2}$$

Considering the second sum boundaries, y and r become, with $r = r_0$

$$\frac{2}{3\delta^2}\left(r_0^2 - y_1^2\right)^{3/2} = \frac{2r_0^3}{3\delta^2}\sin^3\lambda$$

Hence, using Eq. (52) to get y_1 in terms of R :

$$M_2'' = \frac{4}{3} f\ \tan\alpha\,\frac{t_0}{\delta^2}\left(r_0^2 - y_1^2\right)^{3/2} = \frac{4}{3} f\ \tan\alpha\, t_0\,\frac{r_1^2 \sin^2\lambda}{\delta^2} \tag{56}$$

First term has limit value $\mathfrak{W}'$. It corresponds to the solid section hypothesis which applies up to minimum radius of curvature R'. This can be checked from Eq. (52) and letting $y = r_0$. This limit case shall be referred to as the *critical curvature.*

Thus

$$\frac{r_0}{R'} = \frac{f\tan\alpha}{\xi}\frac{t_0}{Ea}$$

And, consequently :

$$\frac{\mathfrak{W}'}{Ea\delta} = \frac{\pi}{4} f\tan\alpha\left(\frac{r_0}{\delta}\right)^3\frac{t_0}{Ea} \tag{57}$$

In this case, the moment second term vanishes.

Beyond that point, wires are in the slip regime. When slip is complete, wires being completely independent, bending moment reaches a limit value $\mathfrak{W}''$. Such limit state is an asymptotic value. Bending moment tends towards that value as radius R decreases, indicating a decreasing strand incremental resistance to bending.

That limit value is obtained from Eq. (56), by letting $y_1 = 0$. Thus:

$$\frac{\mathfrak{W}''}{Ea\delta} = \frac{4}{3} f \tan\alpha \left(\frac{r_0}{\delta}\right)^3 \frac{t_0}{Ea} \tag{58}$$

Ratio of these limit values is a constant :

$$\frac{\mathfrak{W}'}{\mathfrak{W}''} = 0.58$$

Finally, one should note that moment $\mathfrak{W}''$ is in fact friction moment M_w, which was obtained in Section 6, calculating work dissipation from wire slip. This may be checked by comparing Eqs. (28) and (58), which can be rewritten under the form

$$M_w = \frac{2}{\pi} fT \frac{\sin\alpha}{\cos^3\alpha} r_m \qquad \mathfrak{W}'' = \frac{4}{3} f \frac{\sin\alpha}{\cos^2\alpha} \frac{T}{Z} \frac{r_0^3}{\delta^2} \tag{59}$$

Using Eqs (8) and (12) for compact systems :

$$r_m = \frac{2r_o}{3} \qquad Z\delta^2 = 3r_0^2$$

they are found to have a quite close value.

14. Moment-curvature relationship

As seen, a strand reaction bending moment is dependent on three terms. Variation of these terms has been calculated in the following particular case: a four layer, compact structure, simple strand, made of 6 + 12 + 18 + 24 = 60 wires. Outer radius is $r_0 = 4.5\ \delta$. Using typical values f = 0.15 and $\alpha = 17°$, slip starts at $R' = (4.5\times10^4 / 1.1)\delta$, and it may be considered as complete at $R/\delta = 1000$.

Taking Ea = 500 t_0 , the following table shows intermediate values.

Radius R', which corresponds to critical bending curvature, is slightly above 40000δ. The M_2' and M_2'' values appearing in the first column correspond respectively neither to $\mathfrak{W}'$ nor to zero; albeit differing little from them.

$R/1000\delta$	40	30	20	10	1

$y_1 / \delta = (r_0 / \delta)\cos\lambda$	4.4	3.3	2.2	1.1	0.11
$1000M_1 / Ea\delta$	0.08	0.11	0.16	0.33	3.28
$1000M'_2 / Ea\delta$	6.97	4.93	2.52	0.67	0
$1000M''_2 / Ea\delta$	0.09	3.56	7.52	10.34	11.2
$1000M / Ea\delta$	7.14	8.60	10.20	11.34	14.48
$\theta = MR / Ea\delta^2$	285.6	258	204	113.4	14.5

Second row from bottom is the sum of the three preceding rows, yielding the resulting bending moment M, which corresponds to the strand bending resistance.

Last row is the product of that second row from bottom, by the top row, that is:

$$\frac{MR}{Ea\delta^2} = \theta$$

θ is a factor such that $a\delta^2\theta$ is the strand equivalent moment of inertia for the corresponding imposed curvature.

It should be compared to its lower and upper values. The former corresponds to the complete slip hypothesis, where bending inertia is the sum of individual wire inertia (θ=Z/16). The latter , which corresponds to a solid section, is obtained by adding a term $\frac{1}{2}a\sum zr^2$. In this case, the θ factor is increased by a term $\frac{1}{2}a\sum z\left(\frac{r}{\delta}\right)^2$.

With the above example numerical values, the θ lower and upper bounds are:

$$\theta' = 3.75 \qquad \theta'' = 3.75 + 300$$

θ'' differs slightly from the value shown in the first column. This may result from the fact that radius R is slightly smaller than limit radius R'. Or else, it results from the error made by substituting integrals to finite sums in the M calculation.

θ' is also much smaller than the value shown in the last column. This results from the fact that the latter takes into account the contribution of limit bending tensions $(\Delta t)_0$ arising from tangential friction forces.

The above numerical values are shown graphically in Fig. 9. There, curves M_1 M'_2 M''_2 as well as resultant M are shown vs curvature 1/R.
These curves show the stages of the bending process.

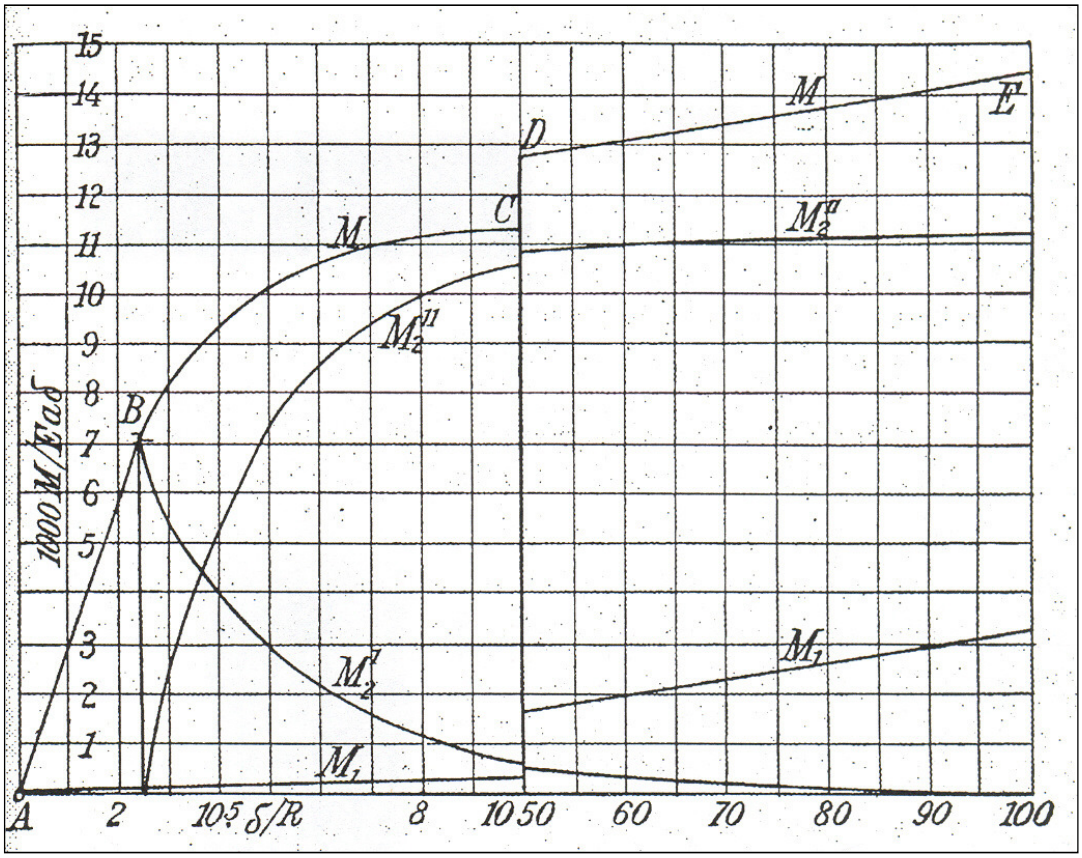

Figure 9

At first, when radius of curvature is large, strand behaves as a solid elastic beam, wires being perfectly bound to one another. There is a linear moment-curvature relationship (straight line *AB*).

When reaching critical curvature, there is impending slip and bending tension diagram (Fig. 8) shows a slope discontinuity: the center part is still a straight line, corresponding to a linear variation with respect to distance from neutral axis; while upper and lower parts of diagram are vertical lines, corresponding to a constant ordinate. These constant tension regions increase as curvature increases.

During this process, the elastic bending moment may be considered as the sum of two separate components, which correspond to both regions of the bending tension diagram: first term, M_2', decreases rapidly as curvature increases, while second term , M_2'', increases rapidly. The sum increases with curvature, though more slowly (curve *BC*).

In the meantime, moment component which arises from independent wire bending (the M_1 term) increases linearly with curvature 1/R. Thus, its diagram is a straight line through the origin. As curvature increases, it becomes more important with respect to the other components. At some point, M_2' is practically zero while M_2'' is almost constant. This explains why curve *DE* (drawn at a different curvature scale in order to extend diagram) corresponds to an M curve which is almost identical to the M_1 curve.

Beyond critical curvature, slip corresponds to some energy dissipation. It is due to friction forces work which has been found in Section 7, where $\mathfrak{X}$ is an equivalent friction force per unit length of strand.

The calculation was based on the inextensible wire hypothesis, which tends to overestimate the friction work as displacements s' from Section 12, should be subtracted from slip s.

This friction work is the main component of the process. In fact, in most of the diagram (in the case of Fig. 9), 9/10 of its span, corresponding to $10^5\ \delta / R$ between 10 and 100), variable moment M_2'' differs very little from its limit value $\mathfrak{M}''$. Recall from Eq. (59) that it is the so-called friction moment.

In the strand bending process, only a small part of the total work (the area under the curve M vs 1/R) corresponds to the increase in the elastic potential, arising from wire axial and bending deformation.

With the elastic moment component M_1 it is easily determined through the formula $\frac{1}{2}\frac{M_1}{R}$.
Increase of elastic potential due to M_2 is the sum of deformation work from wire bending tensions, that is:

$$\frac{(\Delta t)^2\, d\ell}{2Ea} \qquad \frac{(\Delta t)_0^2\, d\ell}{2Ea}$$

They correspond respectively to these parts of the cross-section in which Δt varies linearly, and in which $\Delta t = \Delta t_0 = cst$

With $dx = d\ell \cos\alpha$, and using the corresponding Δt value, it yields:

$$\frac{dL_2'}{dx} = \frac{\xi^2}{\cos\alpha}\frac{Ea}{R^2}\sum_0^{y_1} y^2 \qquad \frac{dL_2''}{dx} = \frac{f^2 \sin\alpha \tan\alpha}{Ea} t_0^2 \sum_{y_1}^{r} y$$

The first summation has already been determined in the calculation of M_2' . It is given by the expression between parentheses in Eq. (55) divided by $4\delta^2$. Hence:

$$\frac{dL_2'}{dx} = \frac{1}{2}\frac{\xi}{\cos\alpha}\frac{M_2'}{R} \tag{60}$$

which confirms the interpretation given for parameter ξ as a warping correction parameter.

Besides, one has the following relationship:

$$\sum_{y_1}^{r} y = \frac{r_0^2}{\delta^2}(\lambda - \sin\lambda\cos\lambda)$$

Indeed, right-hand member is the area of a circular segment, radius r_0 , and central angle $2\lambda = 2\cos^{-1}\left(\frac{y_1}{r_0}\right)$ divided by δ^2. Thus, using Eq. (56):

$$\frac{dL_2''}{dx} = \frac{3}{4}\xi\mu\cos\alpha\frac{M_2''}{R} \tag{61}$$

in which parameter μ is defined as :

$$\mu = \frac{\cos\lambda(\lambda - \sin\lambda\cos\lambda)}{\sin^3\lambda}$$

Using the same data as in the example given at the beginning of this section, typical values of μ are shown in the following table.

$R/1000\delta$	40	30	20	10	1
μ	0.61	0.755	0.464	0.289	0.037

Increase of the elastic potential due to tensions $(\Delta t)_0$ may thus be considered as the work contribution from their bending moment M_2''. Its contribution decreases rapidly as curvature increases, precisely because energy dissipation increases correspondingly.